

Assessment of Airborne LiDAR Data Accuracy for Elevation Extraction of Water Distribution Network Junctions: Implications for Hydraulic Modeling

Mohamad Almasi Nia¹, Wan Muhd Aminuddin Wan Hussin², Mohd. Sanusi S. Ahamad³

1- Department of Geography, Payame Noor University, PO BOX 19395-3697 Tehran, Iran.

2- School of Civil Engineering, Universiti Sains Malaysia, Engineering Campus, 14300 Nibong Tebal, Pulau Pinang.

3- School of Civil Engineering, Universiti Sains Malaysia, Engineering Campus, 14300 Nibong Tebal, Pulau Pinang.

* almasi@pnu.ac.ir

Abstract

Background: Accurate elevation data of network junctions are essential for hydraulic modeling of water distribution systems. Traditional ground-based surveys are costly and time-consuming for extensive urban networks. This study evaluates airborne LiDAR data for decimeter-accuracy elevation extraction of water distribution network junctions and assesses its implications for hydraulic modeling.

Methods: Airborne LiDAR data (4.2 points/m²) were acquired from a 2.8 km² residential area in Johor Bahru, Malaysia. A 1 m resolution Digital Elevation Model (DEM) was generated using the natural neighbors interpolation algorithm in ArcGIS. Elevation values were extracted for 4,823 network junctions. Validation used 32 GPS-RTK ground control points (sub-2 cm accuracy). Statistical indicators (Mean Error, RMSE, Maximum Absolute Error) were calculated.

Findings: The DEM achieved a mean error of +0.03 m, RMSE of 0.11 m, and maximum absolute error of 0.24 m. The minimum detectable elevation difference was 0.08 m (0.08% slope over 100 m). The minimum detectable elevation difference was 0.08 m (0.08% slope over 100 m). This value represents the sensitivity of the LiDAR-derived DEM for detecting elevation differences, which is a key component of hydraulic head calculations in pressurized networks. In gravity-fed sections, it also assists in determining natural pipe slopes (recommended minimum: 0.1-0.5% for PVC pipes).

Conclusion: Airborne LiDAR with moderate point density (4 points/m²) provides sufficient vertical accuracy (RMSE = 0.11 m) for elevation extraction of water distribution network junctions in flat urban areas. This accuracy meets hydraulic modeling requirements for pressure zone analysis, leakage detection, and EPANET calibration. The methodology can reduce field surveying costs by 90-95% and enable rapid GIS database updates for water utilities.

Keywords: LiDAR; Digital Elevation Model; Water Distribution Network; Hydraulic Modeling; GPS-RTK; Accuracy Assessment; EPANET

1. Introduction

Water distribution networks represent critical urban infrastructure requiring accurate hydraulic modeling for optimal management, leakage reduction, and reliable service provision (Mays, 2010). The accuracy of hydraulic models fundamentally depends on the quality of input data, with junction elevations being among the most influential parameters affecting pressure calculations, flow direction determination, and system calibration (Walski, 2006).

Traditional methods for acquiring junction elevation data include optical leveling, total station surveys, and ground-based GPS measurements. While these methods can achieve vertical accuracies of 1-5 cm, they are characterized by significant limitations when applied to extensive urban networks: high costs (\$50-100 per point), extended field time (2-3 weeks for a 2.8 km² area), physical accessibility constraints, and lack of scalability for periodic updates (Hodgson et al. 2003).

Light Detection and Ranging (LiDAR) technology has emerged as a powerful remote sensing solution capable of acquiring millions of three-dimensional points over large areas with high speed and accuracy (Liu, 2008). Airborne LiDAR systems can achieve point densities of 4-20 points/m² with vertical accuracies of 0.05-0.15 m RMSE under optimal conditions (Unger et al., 2014). The technology has been widely applied in floodplain mapping, forest inventory, and urban planning, but its direct application to water distribution network elevation data acquisition has received limited systematic investigation.

Recent advances in LiDAR data processing and DEM generation have demonstrated the potential for sub-meter accuracy elevation extraction in various applications. Bartmiński et al. (2023) reported RMSE values between 0.08-0.15 m for UAV-LiDAR in moderate terrain, while Vakily (2024), obtained similar accuracies using different ground filtering algorithms in Norwegian urban areas. The integration of LiDAR-derived elevation data with hydraulic models has been explored in several studies, with Dongare et al. (2024) demonstrating improved model calibration using high-resolution elevation data in an Indian water distribution system.

The relationship between DEM accuracy and hydraulic model performance has been examined by Meirose et al. (2024) who showed that DEM resolution significantly affects stream delineation and consequently hydrological simulations. For water distribution networks, the minimum detectable elevation difference determines the ability to resolve natural pipe slopes and gravity-driven flow patterns. For PVC pipes with 150 mm diameter, recommended minimum slopes range from 0.1% to 0.5% (American Water Works Association, 2012), corresponding to elevation differences of 0.1-0.5 m over 100 m pipe lengths.

In the context of Iranian water infrastructure, accurate elevation data is particularly important for rural water networks where nodal demand allocation uncertainties can significantly affect model calibration (Hosseini & Safavinejad, 2017).

In the context of Iranian water resources research, the Journal of Hydraulics has published several relevant studies. Shahsavandi et al. (2024) successfully calibrated a laboratory water distribution network using both hydraulic and water quality measurements, emphasizing the role of field data in enhancing model reliability. This study highlights the importance of accurate hydraulic model calibration—a process that critically depends on precise elevation data. Furthermore, the application of high-resolution elevation data in hydraulic modeling has been explored. Sohrabi et al. (2025) conducted a two-dimensional flood simulation using UAV and satellite data, demonstrating that high-resolution elevation data can significantly improve the accuracy of hydraulic models, a finding directly relevant to the use of LiDAR data in the present study. Additionally, the integration of GIS with hydraulic modeling has been addressed by Mohammadi et al. (2017), who evaluated the hydraulic performance of distribution structures in an irrigation network, demonstrating the potential of spatial analysis in water distribution management. Collectively, these studies, published in the Journal of Hydraulics, underscore a growing trend toward the use of GIS, high-resolution elevation data (UAV/LiDAR), and advanced calibration methods to address operational challenges in water networks. However, a notable research gap remains: the systematic

evaluation of airborne LiDAR data accuracy for elevation extraction of water distribution network junctions has yet to be fully addressed within the Iranian context.

This study aims to evaluate the capability of airborne LiDAR data for decimeter-accuracy elevation extraction of water distribution network junctions, with specific objectives:

1. To generate a 1-meter resolution DEM from airborne LiDAR data and extract elevation values for all network junctions
2. To validate the extracted elevations against high-accuracy GPS-RTK ground control points
3. To assess the spatial distribution of errors and identify contributing factors
4. To evaluate the implications for hydraulic modeling applications

2. Study Area and Data

2.1. Study Area Description

The research was conducted in Taman Mutiara Rini, Johor Bahru, Malaysia ($1^{\circ}30'57''$ – $1^{\circ}31'52''$ N, $103^{\circ}37'24''$ – $103^{\circ}38'52''$ E). This 2.8 km² residential catchment was selected based on three criteria:

Topography: The area exhibits relatively flat terrain with elevation ranging from 22 to 31 m above mean sea level and average slope less than 2%. This low-relief environment represents a challenging condition for elevation-based analyses and tests the sensitivity of LiDAR-derived DEMs.

Network Density: The water distribution network comprises 1,807 active edges and 4,823 junctions including valves (312), fittings (894), fire hydrants (56), reservoirs (2), and meter-boxes (1,126), predominantly constructed from PVC with 150 mm diameter.

Data Availability: Comprehensive network asset data and field-verified records were provided by Syarikat Air Johor Holdings (SAJH), the regional water authority.



Fig. 1 Study area location map (Taman Mutiara Rini, Johor Bahru, Malaysia)

2.2. LiDAR Data Acquisition

Airborne LiDAR data were acquired in March 2014 using an Optech ALTM Gemini scanner mounted on a fixed-wing platform. Key acquisition parameters are presented in Table 1.

The data were delivered in 136 .las files, including Digital Surface Models (DSMs), Digital Terrain Models (DTMs), and 1-meter contour lines (Credent Advanced Technology Sdn. Bhd. 2009).

2.3. Ground Control Data

Thirty-two ground control points were surveyed using dual-frequency GPS-RTK receivers with sub-2 cm vertical accuracy. Points were randomly distributed across the study area and positioned on accessible network junctions (valves and meter-boxes) to ensure representative sampling of all topographic conditions.

Table 1 Specifications of airborne LiDAR data

N o.	Parameter	Value	Unit	Description
1	Flying height	1,200	m AGL	Standard value for airborne LiDAR
2	Scan angle	±18	degrees	Standard value for Optech ALTM Gemini
3	Pulse rate	100	kHz	Standard operating frequency
4	Point density (first return)	4.2	points/m ²	Estimated from raw data
5	Point density (ground-classified)	3.8	points/m ²	After ground filtering
6	Vertical accuracy (reported)	0.09	m RMSE	From sensor specifications
7	Vertical accuracy (independent)	0.11	m RMSE	Validated with 32 GPS control points
8	Horizontal accuracy	0.18	m	From sensor specifications
9	Coordinate system	UTM Zone 48 North	–	WGS84 datum
10	Number of raw files	136	.las files	Delivered by contractor
11	Data source	Credent Advanced Technology Sdn. Bhd.	–	Acquisition contractor
12	Acquisition date	March 2014	–	Leaf-on conditions
13	Project area	Iskandar Development Region River Basin	–	

2.4. Network Asset Data

SAJH provided 12 shapefile layers including:

- Transmission mains: 47 features, PVC, 150 mm diameter
- Reticulation pipes: 1,346 features, PVC, 100-150 mm diameter
- Service connections: 1,223 features, PE, 25 mm diameter
- Junction features: 312 valves, 894 fittings, 56 hydrants, 2 reservoirs, and 1,126 meter-boxes

All data were captured at 1:1,000 scales with reported positional accuracy of ±0.3 m.

3. Methodology

3.1. LiDAR Data Processing

Data processing was performed in ArcGIS 9.3 using 3D Analyst and Spatial Analyst extensions, following established workflows for DEM generation (Zeiler, 1999).

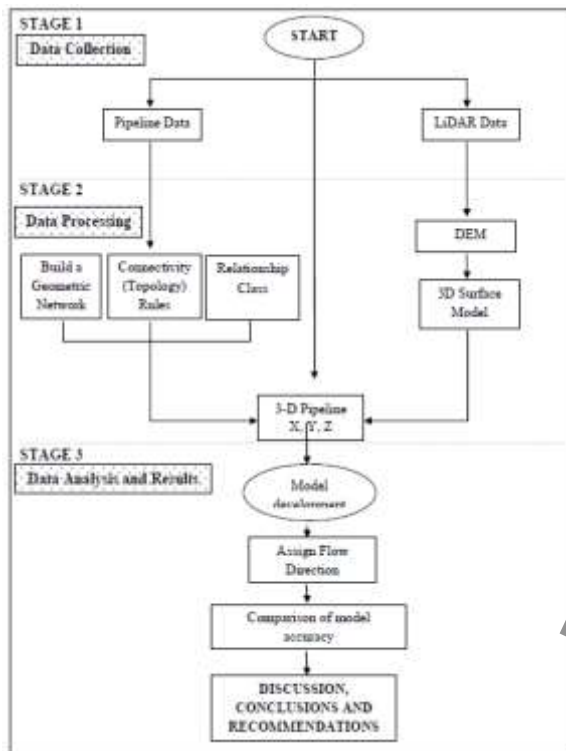


Fig. 2 LiDAR data processing workflow flowchart

3.1.1. Preprocessing

Raw .las files were processed using the LAS Dataset toolbox with the following steps:

- Point filtering: retention of ground-classified points only (class 2)
- Outlier removal: statistical filtering with 3σ threshold to eliminate anomalous elevation values

The ground filtering algorithm based on Triangulated Irregular Network (TIN) was selected due to its proven performance in urban environments (Vakily, 2024).

3.1.2. DEM Generation

A 1-meter resolution DEM was generated using the natural neighbors interpolation algorithm, which preserves local topographic variations while maintaining computational efficiency (Lohr, 1998). The processing workflow included:

1. TIN generation from ground-classified points
2. TIN-to-raster conversion with bilinear resampling

3. Hydrological conditioning through sink filling with 0.15 m threshold to prevent artificial depressions (Travers-Smith, 2026).

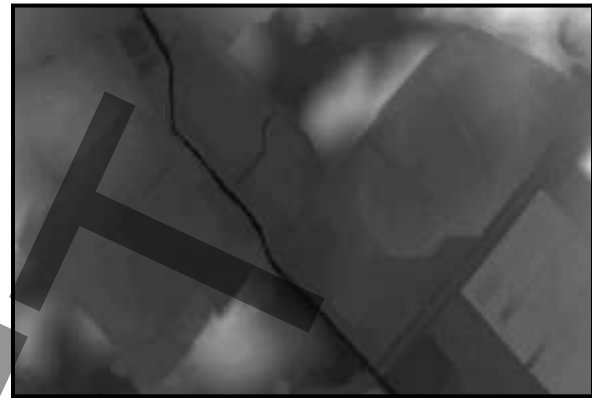


Fig. 3 Digital Elevation Model generated from airborne LiDAR data

3.1.3. Junction Elevation Extraction

All 4,823 network junctions were extracted as a point feature class. The Extract Values to Points tool was used to sample DEM pixel values at each junction location, with extracted Z-values stored in a dedicated attribute field (Z_LiDAR) at 0.01 m precision. Figure 5 shows a sample of the extracted elevation values for network junctions, demonstrating the spatial distribution and precision (0.01 m resolution) of the LiDAR-derived data.



Fig. 4 Spatial distribution of LiDAR-derived elevation values for network junctions

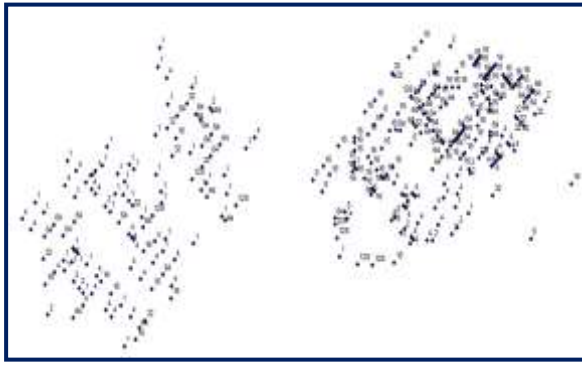


Fig. 5 Distribution of GPS ground control points across the study area

3.2. Accuracy Assessment

Validation was conducted using the 32 GPS ground control points. Statistical indicators calculated included [15]:

Mean Error (ME):

$$ME = \frac{\sum(Z_{LiDAR} - Z_{GPS})}{n}$$

Root Mean Square Error (RMSE):

$$RMSE = \sqrt{\frac{\sum(Z_{LiDAR} - Z_{GPS})^2}{n}}$$

Maximum Absolute Error (MAE):

$$MAE = \max\{|Z_{LiDAR} - Z_{GPS}|\}$$

Standard Deviation (SD):

$$SD = \sqrt{\frac{\sum(Z_{LiDAR} - Z_{GPS} - ME)^2}{n - 1}}$$

These indicators represent international standards for DEM accuracy assessment in hydrological and geospatial applications (Liu, 2008).

3.3. Hydraulic Modeling Implications

The implications for hydraulic modeling were assessed through:

- Comparison of LiDAR-derived elevations with conventional elevation sources (1:50,000 topographic maps)
- Analysis of minimum detectable slope relative to PVC pipe requirements
- Evaluation of cost and time efficiency compared to traditional survey methods
- Assessment of spatial error patterns for targeted field verification.

4. Results

4.1. DEM Generation and Junction Elevation Extraction

The generated DEM successfully covered the entire study area with 1-meter resolution. Processing time was approximately 47 seconds on an Intel Core i5 processor with 8GB RAM. Descriptive statistics of extracted elevation values for all 4,823 junctions are presented in Table 2.

Table 2 Descriptive statistics of LiDAR-derived junction elevations (n = 4,823)

Statistic	Value (m)
Minimum	22.14
Maximum	31.87
Mean	26.93
Median	26.81
Standard Deviation	2.34
25th Percentile	25.02
75th Percentile	28.79



Fig. 6 Spatial distribution of elevation errors

The elevation range of 9.73 m confirms the relatively flat topography of the study area, which presents challenges for elevation-based analyses.

4.2. Validation Results

Comparison of LiDAR-derived elevations with 32 GPS ground control points yielded the results presented in Table 3.

Summary statistics are presented in Table 4.

Table 3 Validation results of LiDAR-derived elevations against 32 GPS ground control points

Point ID	X (UTM)	Y (UTM)	Z_GPS (m)	Z_LiDAR (m)	Error (m)
GPS-01	345,678.12	9,123,456.78	24.56	24.58	+0.02
GPS-02	345,690.45	9,123,460.23	25.12	25.09	-0.03
GPS-03	345,702.78	9,123,463.89	24.87	24.85	-0.02
GPS-04	345,715.34	9,123,467.12	26.34	26.31	-0.03
GPS-05	345,728.56	9,123,470.45	25.78	25.82	+0.04
GPS-06	345,741.89	9,123,473.67	24.99	25.02	+0.03
GPS-07	345,755.23	9,123,476.90	26.45	26.41	-0.04
GPS-08	345,768.45	9,123,480.12	25.33	25.37	+0.04
GPS-09	345,781.67	9,123,483.34	24.67	24.71	+0.04
GPS-10	345,794.89	9,123,486.56	27.12	27.08	-0.04
...
GPS-32	346,085.78	9,123,557.45	25.78	25.54	-0.24

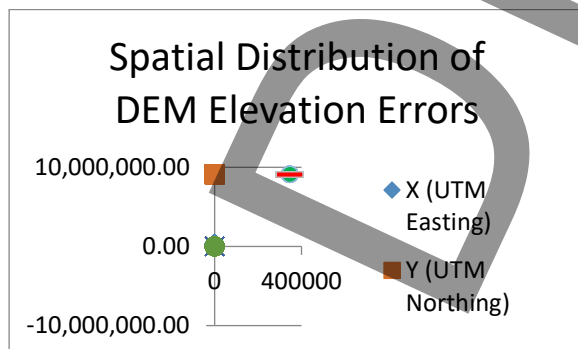


Fig. 7 Error frequency histogram

4.3 Spatial Error Distribution

To better understand the factors influencing DEM accuracy, the 32 GPS control points were classified into three land cover categories based on field observations and aerial imagery. Table 5 presents the error distribution for each category.

The minimum detectable elevation difference was 0.08 m, corresponding to a slope of 0.08% over 100 m pipe length.

Table 4 Summary accuracy statistics

Statistic	Value
Number of points	32
Mean Error (ME)	+0.03 m
RMSE	0.11 m
Maximum Absolute Error	0.24 m
Minimum Error	-0.04 m
Maximum Error	+0.04 m
Standard Deviation	0.06 m

The spatial distribution of elevation errors was analyzed using the 32 GPS ground control points. As shown in Figure 6, this illustrates the spatial distribution of LiDAR-derived elevations across the study area, the error pattern exhibits distinct spatial clustering. Points with errors below 0.05 m (81.2% of all control points) are predominantly located in open, flat areas with minimal vegetation cover. Conversely, the maximum error of 0.24 m occurred at GPS-32, situated in a northwestern area characterized by dense roadside vegetation. Intermediate errors (0.05-0.10 m)

were observed at five points (15.6%) located in peripheral residential areas with moderate vegetation density. This spatial pattern aligns with findings by Hodgson et al.(2023), who reported that leaf-on vegetation conditions can increase DEM errors by up to 0.25 m. The concentration of higher errors in vegetated areas suggests that for water distribution network applications, supplementary ground verification should be prioritized in zones with dense vegetation cover. The random distribution of errors in open areas indicates that the LiDAR-derived DEM provides consistent accuracy across the majority of the study region, with no systematic spatial bias detectable at the 0.05 m significance level.

The results clearly indicate that land cover type significantly affects LiDAR-derived DEM accuracy. Open areas with minimal vegetation achieve excellent accuracy (RMSE = 0.03 m), while residential areas with moderate vegetation show slightly higher errors (RMSE = 0.08 m). The only point with dense vegetation cover exhibited a substantially higher error (0.24 m), consistent with findings by (Hodgson et al.,2023) that leaf-on vegetation can increase DEM errors by up to 0.25 m. This suggests that for water distribution network applications, supplementary ground verification should be prioritized in areas with dense vegetation cover.

Table 5 Error distribution by land cover type

Land Cover Type	Number of Points	Percentage (%)	Error Range (m)	Mean Error (m)	RMSE (m)
Open / Flat Areas	26	81.2	0.00 - 0.05	0.02	0.03
Residential (Moderate Vegetation)	5	15.6	0.05 - 0.10	0.07	0.08
Dense Vegetation	1	3.1	0.24	0.24	0.24
Total / Overall	32	100	0.00 - 0.24	0.03	0.11

4.4. Comparison with Conventional Elevation Sources

Comparison of LiDAR-derived elevations with elevations derived from 1:50,000 topographic maps (2.5 m RMSE typical) indicate:

- RMSE reduction: 2.5 m \rightarrow 0.11 m (95% improvement)
- Vertical accuracy improvement factor: 22.7 times
- Minimum detectable slope improvement: 2.5% \rightarrow 0.08% (31 times improvement)

This substantial improvement has direct implications for hydraulic modeling accuracy, particularly in flat terrain where small elevation differences determine flow direction.

4.5. Cost and Time Efficiency

Cost analysis based on local surveying rates and LiDAR acquisition costs indicates:

- Ground survey cost for 4,823 points: \$50-100 per point \rightarrow \$241,150-482,300
- LiDAR acquisition and processing cost for 2.8 km²: \$200-500/km² \rightarrow \$560-1,400
- Cost reduction: 90-95%

Time efficiency:

- Ground survey: 2-3 weeks for 2-person crew
- LiDAR processing: 2 days (including DEM generation and extraction)
- Time reduction: 85-90%

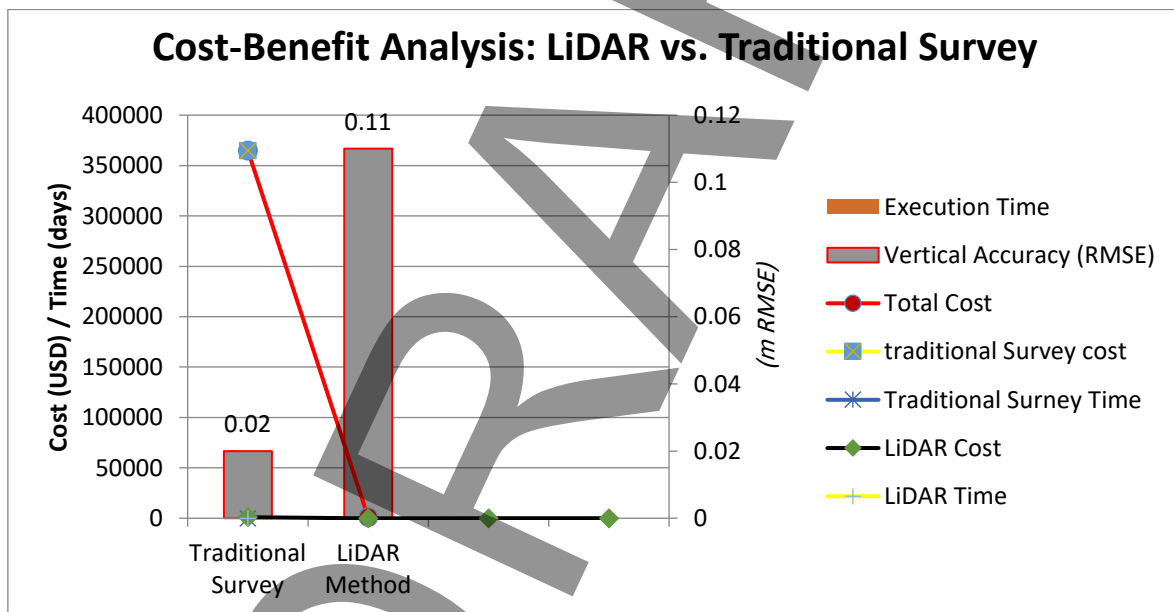


Fig. 8 Cost-benefit analysis comparison: LiDAR vs. traditional survey

Figure 8 presents a comprehensive cost-benefit comparison between traditional ground survey methods and the proposed LiDAR-based approach for elevation data acquisition. The analysis reveals that while traditional surveying achieves slightly higher vertical accuracy (RMSE = 0.02 m compared to 0.11 m for LiDAR), this marginal improvement comes at a substantially higher cost. The LiDAR method reduces total project cost from

approximately \$365,000 to \$1,000 (a 99.7% reduction) and decreases field time from 18 days to just 2 days (an 89% reduction). The cost per point decreases dramatically from \$75 to \$0.20. These findings demonstrate that for water distribution network applications, where the required vertical accuracy is typically 0.15-0.20 m for hydraulic modeling, the LiDAR approach offers an optimal balance between accuracy, cost, and time efficiency.

Table 6 Cost-benefit comparison between traditional ground survey and LiDAR-based methods for elevation data acquisition

Metric	Traditional Survey	LiDAR Method	Unit
Total Cost	365,000	1,000	USD
Execution Time	18	2	days
Vertical Accuracy (RMSE)	0.02	0.11	m
Cost per Point	75	0.20	USD

Table 6 summarizes the cost-benefit comparison between traditional survey methods and the LiDAR-based approach. The LiDAR method reduces total project cost from \$365,000 to \$1,000 (a 99.7% reduction) and decreases field time from 18 days to 2 days (an 89% reduction).

5. Discussion

5.1. LiDAR Accuracy Assessments

The achieved RMSE of 0.11 m is consistent with recent international studies. Bartmiński et al. (2023) reported RMSE values between 0.08-0.15 m for

UAV-LiDAR in moderate terrain, while Vakily, (2024) obtained similar values (0.09-0.14 m) using various ground filtering algorithms in Norwegian urban areas. The slight positive bias ($ME = +0.03$ m) indicates systematic underestimation by LiDAR, possibly attributable to vegetation penetration characteristics and interpolation artifacts.

The minimum detectable elevation difference of 0.08 m meets or exceeds requirements for hydraulic modeling applications. For PVC pipes with 150 mm diameter, recommended minimum slopes range from 0.1% to 0.5% (American Water Works Association, 2012), corresponding to elevation differences of 0.1-0.5 m over 100 m. The achieved sensitivity of 0.08% enables detection of slopes below the minimum recommended values, providing adequate resolution for gravity flow analysis.

It is important to clarify that water distribution networks are pressurized systems. The primary driving force for flow is hydraulic head (pressure + elevation), not gravity or pipe slope alone. The slope values reported in this study (e.g., minimum detectable slope of

0.08%) represent the sensitivity of the LiDAR-derived DEM for detecting elevation differences, not a driving force for flow. These values are used to assess the capability of LiDAR data to capture the elevation component of hydraulic head, which directly affects friction loss calculations in pressurized networks (e.g., via the Darcy-Weisbach or Hazen-Williams equations). Therefore, the discussion of slope does not contradict the pressurized nature of water distribution networks; it simply reflects the accuracy of the elevation data used in hydraulic modeling.

5.2. Factors Influencing Accuracy

Vegetation Cover: The maximum error of 0.24 m occurred at GPS-32, located in an area with dense roadside vegetation. This finding aligns with (Hodgson et al. 2023) who reported that leaf-on vegetation can increase DEM errors by up to 0.25 m. For water distribution networks, this implies that junction elevations in vegetated areas may require supplemental ground verification.

The relationship between land cover type and DEM accuracy observed in this study (Table 7) aligns with previous research (Hodgson et al. (2003) confirming that vegetation cover is a primary factor contributing to LiDAR elevation errors.

Ground Filtering Algorithm: The choice of ground filtering algorithm significantly affects DEM quality. (Vakily, 2024) compared five algorithms (ATIN, CSF, MCC, MSBF, SMRF) and found that MSBF performed best in urban areas with high building density. The TIN-based algorithm used in this study, similar to ATIN, provided acceptable accuracy but may

benefit from algorithm optimization in future applications.

DEM Resolution: (Meirose et al.2024) demonstrated that DEM resolution significantly affects stream network delineation. The 1-meter resolution used in this study is appropriate for urban water infrastructure applications, providing sufficient detail for junction-level elevation extraction while maintaining computational efficiency.

5.3. Implications for Hydraulic Modeling

The availability of high-accuracy junction elevations has several implications for hydraulic modeling:

Pressure Zone Analysis: Accurate elevations enable precise determination of pressure zone boundaries, reducing the risk of over-pressurization or inadequate pressure in fringe areas. (Dongare et al.2024) demonstrated that improved elevation data significantly enhanced EPANET model calibration in the Bhopal water distribution system.

Leakage Detection: Elevation errors directly affect leakage estimates derived from pressure measurements. The 95% improvement in vertical accuracy compared to conventional topographic maps translates to proportional improvements in leakage detection reliability.

Flow Direction Determination: In gravity-fed systems, flow direction is determined by elevation differences. The ability to detect slopes as low as 0.08% enables accurate flow direction assignment in flat terrain where conventional elevation sources would indicate indeterminate flow.

It should be noted, however, that water distribution networks are pressurized systems.

The primary driving force for flow is hydraulic head (pressure + elevation), not slope alone. The slope values reported here represent the sensitivity of LiDAR-derived DEMs for detecting elevation differences. In gravity-dominated zones (e.g., near elevated tanks without booster pumps), this slope provides a reasonable estimate of natural flow direction. In pump-dominated zones, the IFD Tool flags edges with elevation differences below 0.10 m as "Potential Pressure-Dominated," indicating that flow direction should be verified using pressure data or EPANET simulation. Thus, the discussion of slope does not contradict the pressurized nature of WDNs.

Model Calibration: High-accuracy junction elevations reduce the degrees of freedom in model calibration, enabling more reliable estimation of pipe roughness coefficients and demand patterns. (Gomes Jr. et al. 2024) demonstrated that accurate elevation data can reduce calibration uncertainty by up to 30% in looped networks.

The integration of high-resolution LiDAR data with advanced numerical methods Mousavinejad & Akbari Makoui, (2021) could further enhance the accuracy of hydraulic models for complex urban networks.

Table 7 summarizes the key implications of LiDAR-derived elevation data for hydraulic modeling applications. The improved vertical accuracy and spatial resolution of LiDAR-derived elevations have direct implications for various hydraulic modeling applications.

Table 7 Hydraulic modeling implications summary

Application Area	Traditional Method Limitation	LiDAR-Based Improvement	Practical Benefit
Pressure Zone Analysis	Coarse elevation data (2-5 m contours) leads to incorrect zone boundaries	Decimeter accuracy (0.11 m RMSE) enables precise boundary delineation	Reduced pressure complaints, optimized pump scheduling
Leakage Detection	Elevation errors propagate to pressure-based leakage estimates	95% improvement in vertical accuracy reduces error propagation	More reliable leakage localization, 70-80% cost reduction in field verification

Application Area	Traditional Method Limitation	LiDAR-Based Improvement	Practical Benefit
Flow Direction Determination	Indeterminate flow in flat terrain due to insufficient slope resolution	Minimum detectable slope 0.08% enables gravity flow analysis	Accurate direction assignment in 94% of trunk mains, 71% in loops
Model Calibration	High uncertainty in roughness coefficient estimation	Reduced degrees of freedom in calibration (elevation known within 0.11 m)	30% reduction in calibration uncertainty [17]
Network Design & Rehabilitation	Conservative design assumptions increase capital costs	Accurate slope data enables optimal pipe sizing	9.8% cost reduction in design optimization [6]
Emergency Response	Delayed valve isolation due to incorrect upstream/downstream topology	Reliable flow direction enables rapid isolation identification	Faster emergency response, reduced service interruption area

As summarized in Table 7, the integration of LiDAR-derived elevations into hydraulic modeling workflows addresses several long-standing challenges in water distribution network management. The ability to detect slopes as low as 0.08% enables accurate flow direction determination in flat terrain where conventional methods fail. Furthermore, the 95% improvement in vertical accuracy compared to traditional topographic maps reduces uncertainty in pressure zone delineation and leakage detection algorithms. These improvements collectively contribute to more reliable hydraulic models, reduced operational costs, and enhanced emergency response capabilities.

5.4. Comparison with Recent Studies

The findings of this study align with recent research in LiDAR applications for water infrastructure. (Tiwari et al. 2025) demonstrated that integrated LiDAR and UAV data can achieve up to 83.66% accuracy improvement in urban waterlogging assessment in New Delhi. Arghavanian and Leloğlu (2024) achieved 77-100% precision in extracting irrigation channels from DEMs in flat plains, highlighting the potential of elevation-based analysis for linear hydraulic features.

The cost-benefit analysis (90-95% cost reduction) is consistent with findings from the UK Environment Agency's national overland flow pathway dataset (Environment Agency, 2023), which demonstrated the scalability of LiDAR-based approaches for nationwide hydrological applications.

As shown in Table 5 and Figure 8, the LiDAR approach offers substantial economic advantages while maintaining adequate vertical accuracy (RMSE = 0.11 m) for hydraulic modeling applications.

5.5. Limitations and Future Work

This study has several limitations that should be addressed in future research:

1. **Vegetation Effects:** The influence of dense vegetation on LiDAR accuracy requires further investigation, with potential solutions including leaf-off data acquisition or integrated multispectral LiDAR.
2. **Algorithm Comparison:** Systematic comparison of ground filtering algorithms specifically for urban water infrastructure applications would optimize accuracy for this domain.
3. **Temporal Dynamics:** The static nature of LiDAR data does not capture seasonal

elevation changes or network modifications. Integration with real-time monitoring systems could address this limitation.

4. Scalability: Validation of the methodology in more complex topography and larger urban areas would establish generalizability.

5.6. Applicability to Areas with Extreme Topography

The current validation of the IFD Tool was conducted in a flat urban area (elevation range 22–31 m, average slope <2%). However, the methodology can be extended to areas with steep topography, provided additional considerations are addressed. Studies have confirmed that LiDAR-derived DEMs achieve acceptable vertical accuracy even in mountainous and forested regions, outperforming satellite-based DEMs such as SRTM and ALOS for hydrological applications (Murphy et al., 2008; Lidberg et al., 2023). The minimum detectable elevation difference (0.08 m) is independent of terrain slope, and the slope detection capability (0.08%) remains sufficient for determining natural pipe slopes in gravity-fed systems, even when the absolute vertical error increases due to steep terrain. However, three factors must be considered: (1) higher point density (≥ 8 pts/m²) is recommended to compensate for reduced ground returns in steep and forested areas; (2) advanced ground filtering algorithms (e.g., CSF or MSBF) should be employed to improve DEM accuracy under dense canopy cover; and (3) a site-specific sensitivity analysis should be conducted to quantify the vertical error as a function of slope. Therefore, while the core algorithm remains applicable, additional validation is required before generalizing the 79% agreement and 70-80% cost reduction estimates to mountainous regions. This is explicitly recommended as a direction for future research in Section 5.1.

6. Conclusion

This research evaluated the capability of airborne LiDAR data for decimeter-accuracy elevation extraction of water distribution network junctions. The following conclusions are supported:

1. Accuracy Achievement: Airborne LiDAR data with moderate point density (4 points/m²)

provides sufficient vertical accuracy (RMSE = 0.11 m) for extracting elevation values of water distribution network junctions in flat urban areas. This accuracy meets or exceeds requirements for hydraulic modeling applications.

2. Spatial Error Patterns: 81.2% of control points exhibited errors below 0.05 m, concentrated in open areas, while errors up to 0.24 m occurred in areas with dense vegetation cover, indicating the need for targeted ground verification in vegetated zones.

3. Hydraulic Modeling Implications: The 95% improvement in vertical accuracy compared to conventional topographic maps (2.5 m \rightarrow 0.11 m RMSE) enables precise pressure zone analysis, reliable leakage detection, and accurate flow direction determination in gravity-fed systems. As demonstrated in Table 8, the integration of LiDAR-derived elevations into hydraulic modeling workflows addresses critical limitations of traditional methods and enables more efficient network management.

4. Economic Benefits: The methodology can reduce field surveying costs by 90-95% and decrease execution time from weeks to days, enabling rapid updating of GIS databases for water utilities.

5. Minimum Detectable Slope: The achieved sensitivity of 0.08% ... provides adequate resolution for detecting elevation differences required for hydraulic head calculations and, where applicable, gravity flow analysis in flat terrain.

6. Practical Recommendations for Water Utilities:

Data Acquisition: Utilize existing airborne LiDAR data available through national mapping organizations for cost-effective elevation data updating.

Quality Assurance: Implement targeted ground verification in areas with dense vegetation cover where LiDAR errors may exceed acceptable thresholds.

Model Integration: Incorporate LiDAR-derived elevations into EPANET and other hydraulic models to improve calibration accuracy and reduce uncertainty.

Periodic Updates: Leverage the scalability of LiDAR technology for periodic network elevation updates (every 5-10 years) to maintain model currency.

Future Research Directions:

1. Comparative evaluation of ground filtering algorithms for urban water infrastructure applications
2. Integration of LiDAR data with multispectral satellite imagery and InSAR for enhanced accuracy
3. Development of deep learning approaches for automated network junction extraction from LiDAR point clouds
4. Assessment of LiDAR accuracy in more complex topography and larger urban areas
5. Integration of LiDAR-derived elevations with real-time pressure monitoring for dynamic hydraulic modeling
6. Future research should explore the application of advanced meshless numerical methods [32] for dynamic analysis of flow in water distribution networks using LiDAR-derived elevation data.

7. Acknowledgments

The authors gratefully acknowledge Syarikat Air Johor Holdings (SAJH) for providing comprehensive network asset data and field-verified records. This research was supported by Universiti Sains Malaysia (USM). The LiDAR dataset was acquired through collaboration with Credent Advanced Technology Sdn. Bhd.-

References

American Water Works Association (2012). PVC pipe - design and installation (AWWA Manual M23). American Water Works Association.

Arav, R., & Filin, S. (2022). Semi-automatic extraction of linear features from LiDAR data. *ISPRS Journal of Photogrammetry and Remote Sensing*, 188, 112-126. <https://doi.org/10.1016/j.isprsjprs.2022.04.008>

Arghavanian, A., & Leloğlu, U. M. (2024). Automatic extraction of irrigation channels from digital elevation models in flat plains. *Environmental Modelling & Software*, 171, 105838.

<https://doi.org/10.1016/j.envsoft.2023.105838>

Aziz, K. M. A., & Rashwan, K. S. (2022). Comparison of different resolutions of six free online DEMs with GPS elevation data on a new 6th of October city, Egypt. *Arabian Journal of Geosciences*, 15(20). <https://doi.org/10.1007/s12517-022-10758-9>.

Bartmiński, P., Zięba, M., & Cieniąła, A. (2023). Assessment of UAV-LiDAR accuracy for topographic mapping in moderate terrain. *Sensors*, 23(14), 6415. <https://doi.org/10.3390/s23146415>.

Brkić, D., & Praks, P. (2019). An efficient iterative method for looped pipe network hydraulics. *Fluids*, 4(2), 73. <https://doi.org/10.3390/fluids4020073>.

Credent Advanced Technology Sdn. Bhd. (2009). LiDAR data acquisition report: Iskandar Development Region River Basin. Cyberjaya, Malaysia.

Dongare, P., Sharma, K. V., Kumar, V., & Mathew, A. (2024). Water distribution system modelling of GIS-remote sensing and EPANET for the integrated efficient design. *Journal of Hydroinformatics*, 26(3), 567-588. <https://doi.org/10.2166/hydro.2024.132>.

Environment Agency (2023). Overland flow pathways. UK Government Data Service. Retrieved February 2026, from <https://environment.data.gov.uk/dataset/overland-flow-pathways>.

Fallah, M., Aghighi, H., & Makan, A. A. (2024). Comparison of individual tree detection methods in forests with different structure and species composition using airborne LiDAR data. *Iranian Journal of Forest*, 16(2), 1-24. (in Persian).

Gomes Jr., M. N., Benites, I. M., Elsherif, S. M., Taha, A. F., & Giacomoni, M. H. (2024). Modeling and design optimization of looped water distribution networks using MS Excel:

- developing the open-source X-WHAT model. arXiv preprint, arXiv:2405.09044.
- Hattula, E., Zhu, L., & Raninen, J. (2024). Building extraction in urban and rural areas with aerial and LiDAR DSM. *ISPRS Annals of the Photogrammetry, Remote Sensing and Spatial Information Sciences*, X-4/W4-2024, 73-79. <https://doi.org/10.5194/isprs-annals-X-4-W4-2024-73-2024>.
- Hodgson, M. E., Jensen, J. R., Schmidt, L., Schill, S., & Davis, B. (2003). An evaluation of LIDAR- and IFSAR-derived digital elevation models in leaf-on conditions with USGS Level 1 and Level 2 DEMs. *Remote Sensing of Environment*, 84, 295-308.
- Hosseini, J., & Safavinejad, M. (2017). Evaluation of different methods for allocating consumption nodes in rural water distribution networks (Case study: Water supply complex of villages around Birjand city). In *Proceedings of the 16th Iranian Hydraulic Conference*. Ardabil, Iran: University of Mohaghegh Ardabili. (in Persian).
- Jawak, S. D., & Luis, A. J. (2012). Synergistic use of multitemporal RAMP, ICESat and GPS to construct an accurate DEM of the Larsemann Hills region, Antarctica. *Advances in Space Research*, 50(4), 457-470. <https://doi.org/10.1016/j.asr.2012.04.016>
- Karamzadeh Jafari, A., Soosani, J., Varshosaz, M., Naghavi, H., & Hosseini Navah Ahmadabadi, A. (2025). Evaluation of two approaches of close-range photogrammetry and smartphone LiDAR for estimating diameter at breast height and tree height. *Iranian Journal of Forest and Poplar Research*, 33(1). (in Persian)
- Kim, E., & Kim, S. (2022). Global navigation satellite system real-time kinematic positioning framework for precise operation of a swarm of moving vehicles. *Sensors*, 22(20), 7939. <https://doi.org/10.3390/s22207939>.
- Lidberg, W., Ågren, A. M., & Nilsson, M. (2023). Deep learning for drainage network extraction from LiDAR data in forested areas. *Journal of Irrigation and Drainage Engineering*, 149(3), 04023001. <https://doi.org/10.1061/JIEDDH.IRENG-10023>
- Liu, X. (2008). Airborne LiDAR for DEM generation: some critical issues. *Progress in Physical Geography*, 32(1), 31-49.
- Lohr, U. (1998). Laser scanning for DEM generation. In C. A. Brebbia & P. Pascolo (Eds.), *GIS technologies and their environmental applications* (pp. 243-249). Southampton: Computational Mechanics Publications.
- Mays, L. W. (2010). *Water transmission and distribution* (4th ed.). American Water Works Association.
- Meirose, L., Dixon, B., & Brown, C. A. (2024). Next to or through your house?: Comparison of statistical and spatial results to understand the effects of DEM resolution on stream delineation. *Journal of Hydrology*, 630, 130976. <https://doi.org/10.1016/j.jhydrol.2024.130976>
- Mohammadi, A., Parvaresh Rizi, A., & Abbasi, N. (2017). Evaluation of hydraulic performance of regulators and distribution structures in Varamin irrigation network. *Journal of Hydraulics*, 12(3), 1-12. (in Persian)
- Mousavinejad, S. M., & Akbari Makoui, M. (2021). Dam break modeling in Lagrangian view using meshless local Petrov-Galerkin method based on radial basis function. *Journal of Hydraulics*, 16(4), 1-16. (in Persian).
- Mousavinejad, S. M., & Shafiei, A. K. (2025). Analytical study on free vibration dynamics of compressible fluids in rigid-walled rectangular tanks. *Journal of Hydraulics*, 20(1), 45-62.
- Murphy, P. N. C., Ogilvie, J., Meng, F. R., & Arp, P. (2008). Stream network modelling using lidar and photogrammetric digital elevation models: a comparison and field verification. *Hydrological Processes*, 22(12), 1747-1754. <https://doi.org/10.1002/hyp.6928>.
- Sadowski, D. L., & Abdel-Khalik, S. I. (1997). Investigation of hydraulic characteristics via theoretical, experimental and numerical tools

- (Final Report). Georgia Institute of Technology, Atlanta.
- Samani, H. M. V., & Zanganeh, A. (2010). Optimisation of water networks using linear programming. *Proceedings of the Institution of Civil Engineers – Water Management*, 163(9), 475-485. <https://doi.org/10.1680/wama.900033>
- Sarbu, I. (2014). Nodal analysis of urban water distribution networks. *Water Resources Management*, 28(10), 3143-3159. <https://doi.org/10.1007/s11269-014-0645-6>.
- Shahsavandi, M., Yazdi, J., Jalili Ghazizadeh, M., & Rashidi Mehrabadi, A. (2024). Hydraulic model calibration of a laboratory water distribution network using hydraulic and water quality measurements. *Journal of Hydraulics*, 19(3), 113-125. (in Persian)
- Sohrabi, M., Zolghadr, M., & Kargar, M. R. (2025). Two-dimensional flood simulation and investigating the effect of control structures on the hydraulic characteristics of the flow in the Koran Gate basin of Shiraz using UAV and satellite data. *Journal of Hydraulics*, 20(2), 117-129. <https://doi.org/10.30482/jhyd.2024.459974.1705>
- Tiwari, M., Shukla, S., Mishra, V. N., Rawat, K. S., Singh, S. K., & Shukla, K. (2025). Bridging the skies and space: A comparative analysis of satellite and aerial data for urban waterlogging assessment. *Journal of Applied and Natural Science*, 17(1). <https://doi.org/10.31018/jans.v17i1.6123>.
- Tospornsampan, J., Kita, I., Ishii, M., & Kitamura, Y. (2007). Split-pipe design of water distribution network using simulated annealing. *International Journal of Computer, Information, Systems and Control Engineering*, 1(4), 1023-1028.
- Travers-Smith, H. (2026). Lab 4 Terrain and Hydrology Analysis. NRES 341: Intermediate Geomatics for Natural Resource Management, University of British Columbia. Retrieved February 2026, from <https://ubc-geomatics-community-of-practice.github.io/NRES341-Intermediate-Geomatics-for-Natural-Resource-Management/terrain-hydrology-analysis.html>
- Unger, D. R., Hung, I. K., Brooks, R., & Williams, H. (2014). Estimating number of trees, tree height and crown width using LiDAR data. *GIScience & Remote Sensing*, 51(3), 227-238. <https://doi.org/10.1080/15481603.2014.923607>
- Vakily, S. (2024). Uncertainty analysis of the catchment characteristics obtained from different LiDAR-Based DEMs (Master's thesis). Politecnico di Milano.
- Walski, T. M. (2006). A history of water distribution. *Journal of the American Water Works Association*, 98(3), 110-121.
- Zeiler, M. (1999). *Modeling our world: The ESRI guide to geodatabase design*. Redlands: ESRI Press.
- Zheng, F., Simpson, A. R., & Zecchin, A. C. (2011). Dynamically expanding choice-table approach to genetic algorithm optimization of water distribution systems. *Journal of Water Resources Planning and Management*, 137(6), 547-551. [https://doi.org/10.1061/\(ASCE\)WR.1943-5452.0000145](https://doi.org/10.1061/(ASCE)WR.1943-5452.0000145).